Carcinogenesis vol.29 no.12 pp.2360–2368, 2008
doi:10.1093/carcin/bgn241
Advance Access publication October 23, 2008

Suppression of microtubule dynamic instability and turnover in MCF7 breast cancer cells by sulforaphane

Olga Azarenko, Tatiana Okouneva, Keith W.Singletary[1], Mary Ann Jordan and Leslie Wilson*

Department of Molecular, Cellular, and Developmental Biology and the Neuroscience Research Institute, University of California, Santa Barbara, CA 93106, USA and [1]Department of Food Science and Human Nutrition, University of Illinois, Urbana, IL 61801, USA

*To whom correspondence should be addressed. Tel: +1 805 893 2819; Fax: +1 805 893 8094;
Email: wilson@lifesci.ucsb.edu

Sulforaphane (SFN), a prominent isothiocyanate present in cruciferous vegetables, is believed to be responsible along with other isothiocyanates for the cancer preventive activity of such vegetables. SFN arrests mitosis, possibly by affecting spindle microtubule function. A critical property of microtubules is their rapid and time-sensitive growth and shortening dynamics (dynamic instability), and suppression of dynamics by antimitotic anticancer drugs (e.g. taxanes and the vinca alkaloids) is central to the anticancer mechanisms of such drugs. We found that at concentrations that inhibited proliferation and mitosis of MCF7-green fluorescent protein-α-tubulin breast tumor cells by ∼50% (∼15 μM), SFN significantly modified microtubule organization in arrested spindles without modulating the spindle microtubule mass, in a manner similar to that of much more powerful antimitotic drugs. By using quantitative fluorescence video microscopy, we determined that at its mitotic concentration required to inhibit mitosis by 50%, SFN suppressed the dynamic instability of the interphase microtubules in these cells, strongly reducing the rate and extent of growth and shortening and decreasing microtubule turnover, without affecting the polymer mass. SFN suppressed the dynamics of purified microtubules in a similar fashion at concentrations well below those required to depolymerize microtubules, indicating that the suppression of dynamic instability by SFN in cells is due to a direct effect on the microtubules. The results indicate that SFN arrests proliferation and mitosis by stabilizing microtubules in a manner weaker than but similar to more powerful clinically used antimitotic anticancer drugs and strongly support the hypothesis that inhibition of mitosis by microtubule stabilization is important for SFN's chemopreventive activity.

Introduction

Isothiocyanates, such as sulforaphane [SFN, 1-isothiocyanato-4-(methylsulfinyl)butane], are important anticancer phytochemicals that exist in the form of glucosinolate precursors in cruciferous vegetables including broccoli, cauliflower and Brussels sprouts (1,2). SFN significantly reduces the incidence and the rate of development of chemically induced mammary tumors in animal models (3), retards tumor development in human tumor xenograft models (4) and inhibits tumor growth during the initiation, promotion and progression stages of carcinogenesis (5). In humans, epidemiological studies have shown that dietary consumption of vegetables containing isothiocyanates correlates strongly with reduced susceptibility to several kinds of cancer including breast, lung and colon (6,7). High concentrations of isothiocyanates can be achieved in the diet by ingesting cruciferous vegetables. For example, in humans, peak SFN concentrations of ∼2 μM in plasma, serum and erythrocytes were achieved 1 h after ingestion of broccoli sprouts containing 200 μM equivalents of isothiocyanates (8). Similarly, studies in rats have demonstrated that plasma concentrations of ∼20 μM SFN were achieved 1 h after ingesting a single 50 μM dose of SFN (9) and that orally administered SFN was rapidly absorbed (10). In another study, the SFN concentration in human mammary glands reached 60 μM 1 h after ingestion of a single 150 μM dose of SFN (11). These orally achieved concentrations are well within the range in which SFN produces its anticancer effects (12,13).

SFN exerts a large number of actions that may singly or in combination contribute to its chemopreventive activity (14,15). Two well-characterized actions of SFN that are believed to be involved in cancer prevention are the inhibition of Phase I and the induction of Phase II drug metabolism enzymes (16–19). In addition, SFN appears to inhibit angiogenesis, a process critical to later stages of carcinogenesis (20) and exerts anti-inflammatory effects in cancer cells mediated through the inhibition of cyclooxygenase-2 expression (21). SFN also inhibits the activity of histone deacetylase, inhibitors of which are thought to possess chemotherapeutic potential (22).

One of SFN's most important anticancer effects is that it inhibits cancer cell proliferation, blocking cell cycle progression at G_2/M in association with mitotic arrest and induction of apoptosis in several human tumor cell lines (5,23). Mitotic arrest by SFN occurs in association with the formation of aberrant mitotic spindles and, in the presence of concentrations of SFN higher than lowest effective inhibitory concentrations, microtubules depolymerize in human endothelial, breast adenocarcinoma and mouse mammary carcinoma cells (20,24,25). Very recently, SFN has been shown to bind covalently and apparently selectively to tubulin in A549 lung tumor cells (26).

The mechanism by which SFN modulates microtubule function in association with its ability to inhibit proliferation and mitosis is not known. Microtubules possess complex polymerization and dynamic properties. They are non-equilibrium polymers composed of heterodimeric αβ-tubulin subunits. At steady state, they undergo two types of guanosine 5′-triphosphate (GTP) hydrolysis-dependent dynamic behaviors, dynamic instability and treadmilling (27–29). Dynamic instability is the switching between episodes of growth and shortening at microtubule ends (30). Treadmilling, or flux, is the net growth of microtubules at their plus ends and shortening at their minus ends (29). Considerable evidence indicates that the rapid dynamic behaviors of microtubules and the tight regulation of their dynamics are critical for mitosis. At mitosis, highly dynamic microtubules are required for the proper and timely attachment of chromosomes to the mitotic spindle, for the movements of the chromosomes to form the metaphase plate and for creating the tension required for successful transition through the metaphase/anaphase checkpoint (31). Perturbation of microtubule dynamics during mitosis can lead to prolonged mitotic arrest and aneuploidy followed by cell death (32). A number of widely used antimitotic anticancer drugs, such as paclitaxel and the vinca alkaloids, arrest mitosis by suppressing spindle microtubule dynamics (33,34). At high effective concentrations, paclitaxel promotes microtubule polymerization, whereas the vinca alkaloids inhibit it (35). Despite their different effects on the quantity of polymer, both groups of drugs strongly suppress the dynamic behaviors of microtubules at concentrations well below those that change the polymer mass. Suppression of microtubule dynamics in distinct ways, which with most antimitotic drugs is brought about by the binding of only a few drug molecules along the surfaces or at the ends of the microtubules, is critically important to the antimitotic and anticancer mechanisms of action of the drugs (29,36). Thus, we wanted to determine whether the modulation of microtubule dynamics is important for the anticancer activity of SFN.

In the present work, we determined the effects of SFN on microtubule dynamic instability in interphase MCF7 cells stably transfected with green fluorescent protein (GFP)-α-tubulin by using quantitative

Abbreviations: GFP, green fluorescent protein; GI_{50}, concentration required to inhibit cell proliferation by 50%; IC_{50}, concentration required to inhibit mitosis by 50%; MAP, microtubule-associated protein; SFN, sulforaphane.

fluorescence time-lapse microscopy. We found that SFN strongly suppressed dynamic instability in these cells in parallel with inhibition of cell proliferation [concentration required to inhibit cell proliferation by 50% (GI_{50}) = 26 μM] and induction of mitotic arrest [concentration required to inhibit mitosis by 50% (IC_{50}) = 13 μM]. Reduction in microtubule turnover was also observed using tubulin acetylation as a marker for microtubule stability (37). Importantly, the suppressive effects of SFN on the dynamic instability of microtubules reassembled from purified bovine brain tubulin were similar to those on microtubules in living cells, indicating that SFN's effects on dynamics and turnover in cells are most probably due to a direct action on the microtubules. Thus, suppression of microtubule dynamics may play an important role in the ability of SFN to exert its anticancer as well as cancer preventive activity. Our findings provide an insight into the antimitotic mechanism of action of SFN in relation to its ability to inhibit proliferation and arrest mitosis in cancer cells.

Materials and methods

Materials

Chemicals were purchased from Sigma–Aldrich (St Louis, MO) unless otherwise noted. D, L-SFN (LKT Laboratories, St Paul, MN) was dissolved in 100% dimethyl sulfoxide (dimethylsulfoxide) and stored at −20°C. Bovine brain microtubule protein [∼70% tubulin and 30% microtubule-associated proteins (MAPs)] was isolated as described previously (38). MAP-free (>99%) tubulin was purified from MAP-rich protein by phosphocellulose column chromatography (39). Proteins were stored at −70°C until use.

Cell culture

Human MCF7 breast adenocarcinoma cells (American Type Culture Collection # HTB 22, ECACC 86012803 morphology type, Manassas, VA), expressing GFP-α-tubulin (Clontech, Palo Alto, CA) (40), were cultured in 5% CO_2 in standard glucose Dulbecco's Modified Eagle's Medium, with 10% fetal bovine serum (HyClone, Logan, UT), 1% penicillin–streptomycin and non-essential amino acids, at pH 7.3, 37°C.

Cell proliferation

Cells were seeded in six-well plates (6×10^4 cells/2 ml), allowed to adhere for 24 h, then incubated with fresh medium containing vehicle control or the desired SFN concentration for 24, 48 or 72 h, harvested by combining floating and attached cells and released by trypsinization. Viability was assessed by counting live cells with a hemacytometer using trypan blue exclusion assay. GI_{50} value (growth/proliferation inhibition by 50%) was calculated by counting live and dead cells as $100 \times (T_{drug}-T_0)/(T_c-T_0) = 50$, where T_{drug} represents the total cell number in the presence of SFN at 24, 48 or 72 h, T_0 is the total cell number at time 0 and T_c is the number of cells in controls at 24, 48 or 72 h. The stated GI_{50} is the average of the GI_{50}s determined by the linear extrapolation for each of three experiments.

Mitotic arrest

Cells were incubated with SFN for 20 h; both floating and attached cells were collected and fixed in 10% formalin (25°C, 30 min), followed by methanol (4°C, 10 min) (41). Fixed cells were mounted on glass slides using ProLong Gold antifade agent with 4′,6-diamidino-2-phenylindole (Invitrogen, Carlsbad, CA) to visualize DNA and examined by fluorescence microscopy (Nikon Eclipse E800, Melville, NY). The percentage of mitotic cells was determined by counting at least 500 cells total for each condition.

Image acquisition and analysis of microtubule dynamics in living MCF7-GFP-α-tubulin cells

Cells were seeded on coverslips for 24 h and incubated with the vehicle control or SFN for 20 h. Live interphase cells were examined and time-lapse images recorded as described previously (41). The positions of the microtubule plus ends were tracked and graphed as microtubule length versus time (life history plots), and the dynamic instability parameters were determined. Briefly, changes in length of ≥0.5 μm between two points were considered growth or shortening events. Changes in length of <0.5 μm were considered periods of attenuated or paused dynamics. The catastrophe frequency is the frequency of transition from the growth or paused state to shortening. Rescue is the frequency of transition from shortening to growth or pause. Dynamicity is the total length grown and shortened divided by the total life span of the microtubule.

Immunofluorescence microscopy and analysis of microtubule turnover by monitoring acetylated microtubules

Cells were seeded on poly-L-lysine-treated coverslips at 6×10^4 cells/2 ml for 24 h, incubated with SFN (24 h), fixed in 10% formalin in phosphate-buffered saline (20 min, 25°C) followed by 10 min in methanol (4°C), washed with phosphate-buffered saline and incubated with 1% normal goat serum (30 min). Next, cells were incubated with mouse DM1 anti-α-tubulin (1:1000, Sigma–Aldrich) and rabbit polyclonal anti-pericentrin (1:200, BabCo, Richmond, CA) antibodies (1 h, 37°C), rinsed 3× in phosphate-buffered saline containing 1% bovine serum albumin followed by incubation with goat anti-rabbit Alexa 488 (1:2000, Invitrogen, Molecular Probes®, Carlsbad, CA) and donkey anti-mouse CY3-conjugated (1:1000, Jackson ImmunoResearch Laboratories, West Grove, PA) secondary antibodies for 1 h at 37°C. After washing, coverslips were mounted on the glass slides using ProLong Gold antifade reagent with 4′,6-diamidino-2-phenylindole (Invitrogen, Carlsbad, CA) to visualize DNA and imaged with CoolSNAP HQ digital camera (Photometrics, Tucson, AZ). To analyze the degree of tubulin acetylation, cell were treated and fixed as above. Microtubules were visualized with rabbit anti-α-tubulin primary (1:400, Sigma–Aldrich) and donkey anti-rabbit Rho (1:150, Jackson ImmunoResearch Laboratories) secondary antibodies. Acetylated tubulin was probed with mouse anti-α-acetylated tubulin primary antibody (1:500, Sigma–Aldrich) and secondary goat anti-mouse-fluorescein isothiocyanate-conjugated antibody (1:1000, Sigma–Aldrich).

Flow cytometry

Cell cycle analysis was performed by using a Guava EasyCyte™ analyzer (Guava Technologies, Hayward, CA) with Cytosoft software 2.0. Briefly, cells were seeded at 6×10^4 cells/2 ml for 24 h and incubated in the absence or presence of SFN for 24 h, harvested and fixed in cold 70% ethanol and stained using Guava Cell Cycle Reagent. Results were analyzed on ModFit LT 3.1 software (Verity Software House, Topsham, ME). Early and late apoptotic cells were counted using a Guava Nexin™ kit.

Image acquisition and analysis of the dynamic instability behavior of purified microtubules by video microscopy

The dynamic instability behavior of individual purified microtubules was carried out by video-enhanced differential interference contrast microscopy using a Zeiss IM35 inverted microscope as described previously (42). Briefly, purified tubulin (16 μM) was mixed with sea urchin axonemal seeds and polymerized to steady state (30 min, 35°C) in PMME buffer (87 mM 1,4-piperazinediethane-sulfonic acid, 36 mM 2-morpholinoethanesulfonic acid, 1.8 mM $MgCl_2$, 1 mM ethyleneglycol-bis(aminoethylether)-tetraacetic acid, 1 mM GTP, pH 6.8 in the presence or absence of SFN. Microtubule lengths were measured every 3–5 s, plotted as length versus time and analyzed using Real-Time Measurement software (43).

Results

Effects of SFN on cell proliferation, mitosis and apoptosis in MCF7 breast tumor cells

To examine how SFN perturbed mitotic spindle microtubule organization and function in MCF7-GFP-α-tubulin cells, we first determined the concentration dependence for SFN's ability to inhibit proliferation in relation to inhibition of mitosis in these cells. SFN inhibited cell proliferation in a time- and concentration-dependent manner (Figure 1A) with half-maximal inhibition (the GI_{50}) occurring at 26 μM (24 h), 13 μM (48 h) and 9 μM (72 h). Cells were arrested at prometaphase/metaphase of mitosis (Figure 1B, bars); half-maximal mitotic accumulation occurred at 13 μM SFN (20 h). SFN reduced the ratio of the number of cells in anaphase plus telophase to the number of cells in prometaphase plus metaphase, an indicator of the extent of mitotic arrest, in a concentration-dependent manner from 0.13 in control cells to 0.10 at 5 μM and 0.02 at 15 μM ($P < 0.01$, Student's t-test). At ≥20 μM SFN, there were no cells in anaphase/telophase and thus mitotic progression was completely arrested prior to the metaphase to anaphase transition. Analysis by flow cytometry confirmed that SFN inhibited cell cycle progression at G_2/M. The highest percentage of cells in G_2/M occurred at 25 μM SFN (64.3% compared with 27.6% in controls) (Figure 1C, hatched bars and insert). SFN also induced apoptosis in a time- and concentration-dependent manner (Figure 1D). Fifteen micromolar of SFN (24 h) (Figure 1D, hatched bars) induced significant apoptosis and 30% of the cells were apoptotic at 50 μM SFN (48 h) (Figure 1D, solid bars). In addition, SFN increased the percentage of multinucleate cells from 1.8% in controls to 17% at 35 μM SFN (Figure 1B, filled circles).

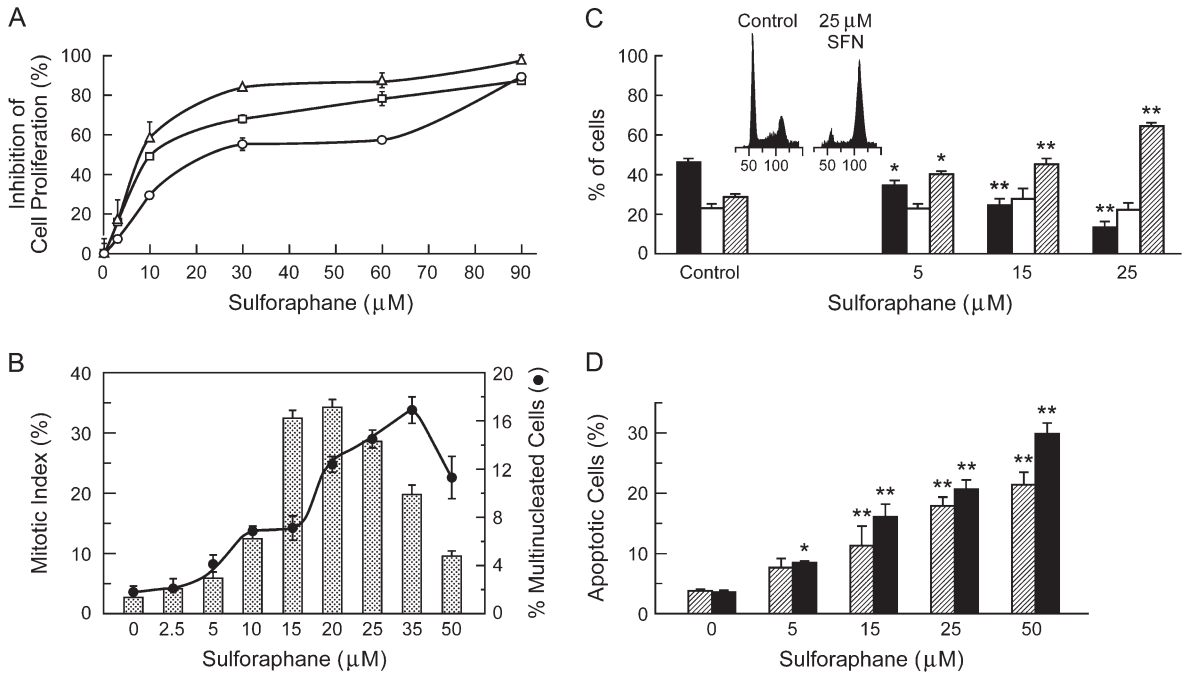

Fig. 1. (**A**) Inhibition of cell proliferation by SFN. Live MCF7-GFP-α-tubulin cells were counted after incubation with a range of SFN concentrations for (open circles) 24, (open squares) 48 and (open triangles) 72 h and GI_{50} calculated as described in Materials and Methods. (**B**) Concentration-dependent accumulation of multinucleate interphase cells (closed circles) and mitotic cells (bars) after incubation with SFN for 20 h (Materials and Methods). (**C**) G_2/M cell cycle arrest induced by SFN. Cells were treated with a range of SFN concentrations for 24 hand analyzed by flow cytometry (Materials and Methods). Solid bars—G_1 phase, open bars—S phase and hatched bars—G_2/M phase of the cell cycle. Insert shows the flow cytometry histograms of controls and cells incubated with 25 μM SFN. The first peak represents G_1 cells and the second peak represents cells in the G_2/M phase of the cell cycle. (**D**) Concentration- and time-dependent induction of apoptosis by SFN. Cells were incubated with a range of SFN concentrations for 24 (hatched bars) and 48 h (solid bars) and the total number of apoptotic cells for each condition was determined by flow cytometry (Materials and Methods). Results are the mean ± SEM of at least four independent experiments performed in duplicate. $^{*}P \leq 0.05$, $^{**}P \leq 0.01$ estimate of significance by Student's *t*-test.

Mitotic spindle organization, chromosome segregation and centrosome orientation

Control cells in mitotic metaphase had normal well-organized bipolar spindles with two well-separated spindle poles and a few astral microtubules. The chromosomes were aligned in a compact equatorial metaphase plate (Figure 2A). At 15 μM SFN (24 h), many spindles were abnormal; only 13% of the spindles were normal and bipolar (data not shown). Most spindles were in a prometaphase-like state and displayed prominent astral microtubules (Figure 2C, arrow) with many of their chromosomes remaining uncongressed at the spindle poles (Figure 2C, arrowheads). At 25 μM SFN, there were no bipolar spindles. Most spindles were monopolar and displayed ball-shaped arrangements of chromosomes with microtubules emanating from the single pole extending well beyond the chromosomes (Figure 2E). At 15 μM SFN, the distance between the poles in bipolar spindles decreased by 39% (7.2 ± 0.1 μm compared with 11.9 ± 0.1 μm in control spindles; $P < 0.01$, Student's *t*-test). At this concentration, the majority of mitotic cells had a pair of centrosomes positioned in the center of an abnormal ball-shaped spindle (Figure 2E). A number of multinucleate interphase cells contained multiple widely separated centrosomes (Figure 2G).

While 15 μM SFN arrested mitosis in these cells, disrupting spindle microtubules, the interphase microtubule network was unaffected. The interphase microtubule network in control cells was organized normally with many distinct microtubules extending from the microtubule-organizing center toward the cell periphery (Figure 2B). Fifteen micromolar SFN did not induce detectable changes in the overall organization and/or mass of microtubules (Figure 2D). However, at SFN concentrations of ≥25 μM, the number of microtubules decreased significantly and they were shorter and/or more curved than microtubules in controls (Figure 2F). Incubation with ≥50 μM SFN resulted in an extensive microtubule loss. Only a few short microtubules remained (e.g. Figure 2H). A significant increase in the number of multinucleate cells was found at ≥10 μM SFN (Figure 2G). These cells may have escaped mitotic arrest and reverted to the interphase condition without completing cytokinesis.

Suppression of dynamic instability and reduction of microtubule turnover in MCF7 cells by SFN

Inhibition of mitosis by most antimitotic anticancer drugs at their lowest effective concentrations occurs by suppression of the dynamics of microtubules rather than by increasing or decreasing the mass of assembled microtubules (35,36,44). Because it is not possible to analyze dynamic instability of individual microtubules in mitotic spindles, we analyzed the effects of SFN on dynamic instability of microtubules in the thin lamellar regions of interphase MCF7-GFP-α-tubulin cells. Most microtubules grew and/or shortened during the course of each control time-lapse sequence. Changing lengths of individual microtubules in control cells and SFN-treated cells (15 μM, 20 h) are shown in Figure 3 Panel IA and B, respectively, and life history traces of individual microtubules are shown in Figure 3 Panel IIA and B, respectively. Most of the microtubules in untreated cells were highly dynamic, whereas the majority of microtubules in cells incubated with SFN were either stable or were minimally dynamic. Such data were used to analyze the effects of SFN on the dynamic instability parameters of individual microtubules (Table I). It is qualitatively clear that SFN stabilized microtubule dynamics. While SFN affected most of the individual dynamics parameters of the microtubules, its strongest effects were to reduce the rate and extent of shortening (Table I; Figure 4 Panel IA and B). Specifically, 15 μM SFN (the IC_{50} for mitotic arrest) reduced the shortening rate by 50% and the shortening length by 57%. It also strongly inhibited the growth rate and length grown during growing excursions by 30 and 49%, respectively (Figure 4 Panel IA and B), and it reduced the overall dynamicity by 53% (Figure 4 Panel IC). In addition, SFN reduced the durations of individual growth and shortening events (data not

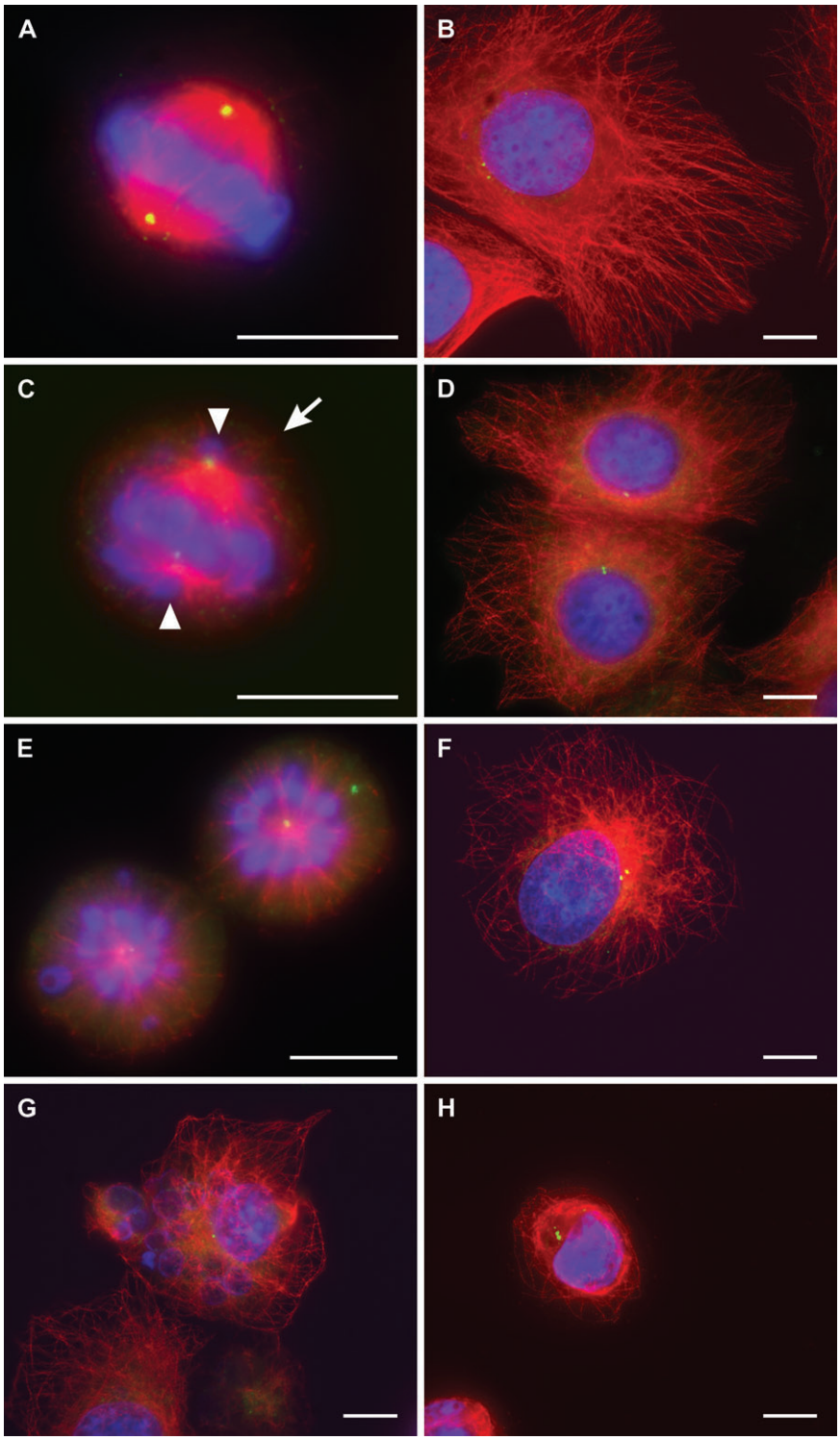

Fig. 2. Effects of SFN on microtubule arrangement, spindle morphology and centrosome orientation in MCF7-GFP-α-tubulin cells. (**A**) Control metaphase cell; (**B**) control interphase cell; (**C** and **D**) cells incubated with 15 μM SFN, 24 h (mitotic and interphase, respectively); an arrow indicates astral microtubules, arrowheads indicate uncongressed chromosomes; (**E**, **F** and **G**) 25 μM SFN, 24 h (mitotic, interphase, multinucleated interphase cell, respectively) and (**H**) 50 μM SFN, 24 h, interphase cell. Chromosomes/nuclei are blue (4′,6-diamidino-2-phenylindole), microtubules are red and centrosomes are green. Bar = 10 μm.

shown). At 2 × IC_{50} for mitotic arrest (25 μM), SFN clearly affected the structure of the fully stabilized microtubules, inducing a high degree of microtubule curvature (Figure 2F).

Posttranslational acetylation of alpha tubulin at lysine 40 is a marker for stable microtubules, which turn over slowly as compared with dynamic microtubules (37). Microtubules with low quantities of acetylated tubulin are dynamic and turn over rapidly, whereas acetylated microtubules turn over slowly or not at all (37). Using anti-acetylated tubulin antibodies, we found that SFN promoted acetylation of interphase microtubules in MCF7-GFP-α-tubulin cells in a concentration-dependent manner, further demonstrating that the microtubules were stabilized by SFN (Figure 5). Control cells had trace amounts of acetylated tubulin (Figure 5, control). Low concentrations of SFN (15 and 25 μM) promoted tubulin acetylation in concert with

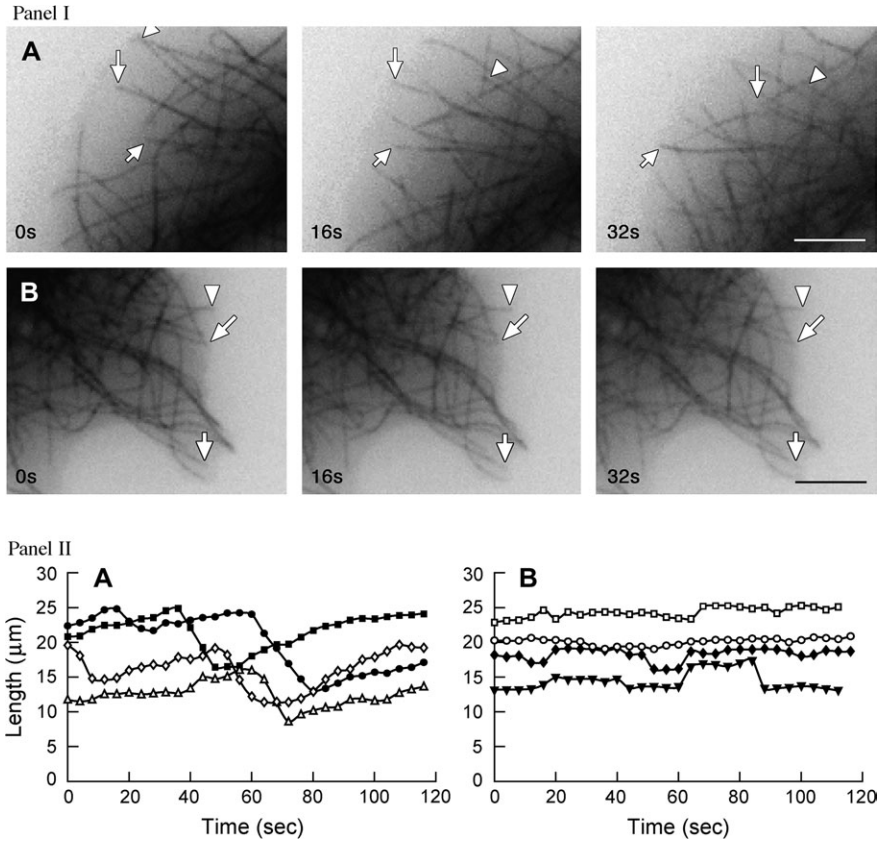

Fig. 3. Panel I: Time-lapse sequences of microtubules in MCF7-GFP-α-tubulin cells in the absence (**A**) and presence (**B**) of 15 μM SFN. Inverted image. Arrows and arrowheads indicate the ends of the dynamic (control cells) and stabilized (treated cells) microtubules that changed their lengths over the course of 32 s. Bar = 5 μm. Panel II: Life history plots of individual microtubules. Time sequences of length changes of individual microtubules at their plus ends in (**A**) control cells and (**B**) cells after incubation with 15 μM SFN for 20 h.

the suppression of microtubule dynamics (Figure 5, acetylated tubulin panel). At high SFN concentrations (≥50 μM SFN), microtubules partially depolymerized and the remaining microtubules became completely stable and highly acetylated compared with those in control cells (Figure 5, 50 μM SFN).

Effects of SFN on polymerization and dynamic instability of purified microtubules

While high concentrations of SFN inhibit microtubule polymerization, we found that the lowest effective SFN concentrations in MCF7-GFP-α-tubulin cells neither inhibited polymerization nor modified the structures of purified microtubules. Specifically, both MAP-free (>99%) and MAP-rich bovine brain tubulin (70% tubulin, 30% MAPs) were polymerized to steady state in the absence or presence of SFN concentrations between 25 and 100 μM (supplementary Figure 1 is available at *Carcinogenesis* Online). As reported previously by Jackson *et al.* (24,25), high concentrations of SFN inhibited polymerization of MAP-free microtubules. However, little, if any, inhibition of assembly occurred at 25 μM SFN and half-maximal inhibition of assembly required ∼70 μM SFN. We also found that the ability of SFN to inhibit polymerization of MAP-rich brain tubulin was even weaker than its ability to inhibit polymerization of purified MAP-free tubulin [$IC_{50} \sim 200$ μM SFN (supplementary Figure 1 is available at *Carcinogenesis* Online)]. By electron microscopy, in the presence of 15 μM SFN, microtubules were indistinguishable from control microtubules (data not shown). High concentrations of SFN (≥50 μM SFN) inhibited tubulin polymerization in association with the formation of tubulin aggregates (data not shown). Thus, SFN concentrations of ≤25 μM, as used in MCF7-GFP-α-tubulin cell experiments, did not appreciably modify the mass or the structure of polymerized microtubules.

We analyzed the effects of SFN on *in vitro* dynamic instability of individual steady-state MAP-free microtubules at their plus ends by differential interference video microscopy at concentrations that did not modify the structure or mass of the microtubules. The growing and shortening dynamics of the microtubules were strongly suppressed by SFN in a manner that was very similar to the effects of SFN on dynamic instability in MCF7-GFP-α-tubulin cells (Table I, Figure 4 Panel II). For example, 15 μM SFN, which had no effect on polymerization (supplementary Figure 1 is available at *Carcinogenesis* Online), decreased the growth rate by 45% from 0.56 ± 0.07 μm/min in controls to 0.31 ± 0.04 μm/min and the length of the microtubules grew by 60% from 1 μM in controls to 0.4 μM. It reduced the shortening rate by 45% from 21.1 ± 4.6 μm/min to 11.8 ± 0.9 μm/min and the shortening length by ∼30% from 4.2 μm to 3 μM (Figure 4 Panel IIA and B). In addition, SFN decreased the percentage of time the microtubules spent growing and increased the percentage of time the microtubules spent in an attenuated state, neither growing nor shortening detectably (Table I). As a result of these changes, the dynamicity (a measure of the total tubulin exchange at plus ends per unit of time) was reduced by 80% at 15 μM SFN (Table I; Figure 4 Panel IIC).

Discussion

We have found that SFN suppresses dynamic instability and decreases the turnover of microtubules in MCF7-GFP-α-tubulin breast cancer cells at concentrations similar to those that inhibit cell proliferation and arrest mitosis. SFN also suppressed the dynamic instability behavior of purified microtubules in a manner similar to that in living cells, indicating that its effects on dynamics in cells were due to a direct action on the microtubules. Importantly, the effects of SFN on

Table I. Modulation of dynamic instability at microtubule plus ends by SFN

Parameter	Concentration (μM)			
	0 (control)	5	10	15
A. Effects of SFN on dynamic instability of microtubules in living interphase MCF7-GFP-α-tubulin breast adenocarcinoma cells[a]				
Rate (μm/min)				
Growth	14.5 ± 1.07	11.2 ± 0.62*	10.1 ± 0.52**	10.1 ± 0.62**
Shortening	22.4 ± 1.7	18.8 ± 0.9*	12.6 ± 1.0**	11.2 ± 0.9**
Length change (μm)				
Growth	3.3 ± 0.31	2.7 ± 0.11	2.1 ± 0.2*	1.7 ± 0.1**
Shortening	4.7 ± 0.6	4.0 ± 0.3*	2.08 ± 0.3**	2.0 ± 0.4**
Attenuation duration (min)	0.27 ± 0.02	0.31 ± 0.04	0.34 ± 0.02*	0.37 ± 0.04*
Time growing (%)	29.5	31.5	28.9	21.7
Time shortening (%)	28.6	28.5	27.8	28.3
Time attenuated (%)	41.9	40.0	43.3	50.0
Catastrophe frequency/min	2.05 ± 0.2	1.88 ± 0.13	1.3 ± 0.11*	0.97 ± 0.13**
Rescue frequency/min	4.4 ± 0.5	3.5 ± 0.4	5.1 ± 0.5*	5.5 ± 0.4**
Dynamicity (μm/min)	10.6 ± 1.1	8.4 ± 0.6	6.2 ± 0.7**	5.0 ± 0.5**
B. Effects of SFN on dynamic instability of steady-state-purified microtubules *in vitro*[b]				
Rate (μm/min)				
Growth	0.56 ± 0.07	0.53 ± 0.02	0.50 ± 0.07*	0.31 ± 0.04**
Shortening	21.1 ± 4.6	17.5 ± 3.7*	12.3 ± 3.3**	11.8 ± 0.9**
Length change (μm)				
Growth	1.0 ± 0.09	0.85 ± 0.11	0.6 ± 0.05*	0.4 ± 0.06**
Shortening	4.2 ± 0.5	3.5 ± 0.2*	3.3 ± 0.1*	3.0 ± 0.1**
Attenuation duration (min)	0.85 ± 0.08	0.95 ± 0.15	1.3 ± 0.13**	1.5 ± 0.04**
Time growing (%)	75.1	68.4	41.4	31.5
Time shortening (%)	5.0	9.1	12.1	12.7
Time attenuated (%)	19.9	22.5	46.5	55.8
Catastrophe frequency/min	0.3 ± 0.06	0.2 ± 0.04	0.3 ± 0.05	0.3 ± 0.07
Rescue frequency/min	3.3 ± 0.9	3.1 ± 0.5	2.8 ± 0.4	2.8 ± 0.4
Dynamicity (μm/min)	1.5	1.1	0.5	0.3

Values are means ± SE, except for the catastrophe and rescue frequencies, which are means ± SD. Values were analyzed for statistical significance and differ significantly from controls at $^{*}P \leq 0.05$, $^{**}P \leq 0.001$, Student's *t*-test.

[a]Dynamicity per microtubule is the length grown and shortened divided by the total life span of the microtubule, values are means ± SE. At least 50–60 microtubules were analyzed for each condition.

[b]Tests of significance were not done on dynamicity, an overall variable. At least 25–35 microtubules were analyzed for each condition.

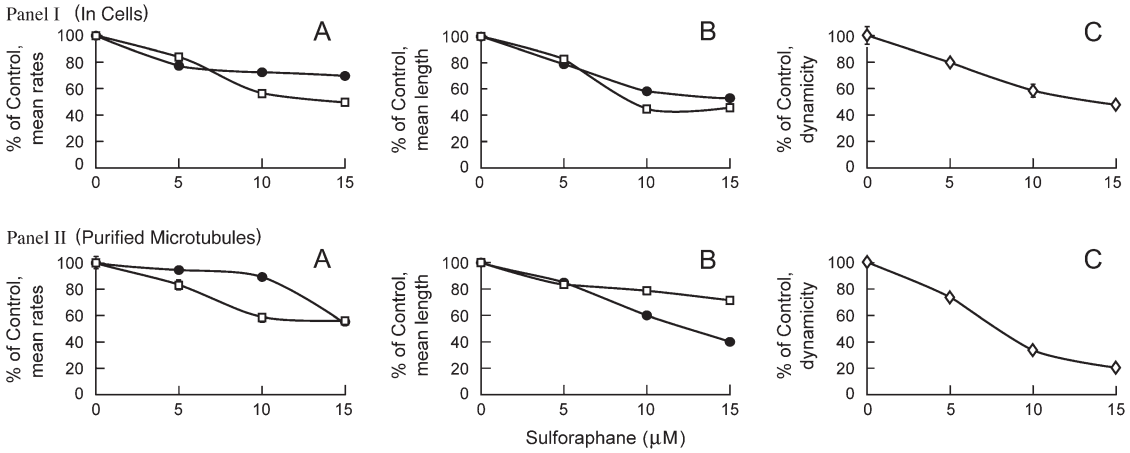

Fig. 4. Concentration dependence for the suppression of growth and shortening rates (**A**), lengths (**B**) and dynamicity (**C**) by SFN; (closed circles) growth, (open squares) shortening and (open diamonds) dynamicity. Panel I, microtubules in living interphase MCF7-GFP-α-tubulin cells and Panel II, purified microtubules assembled from bovine brain tubulin. Results are the mean ± SEM of four or five independent experiments. Error bars in some cases are too small to be seen.

microtubules both in cells and with purified polymers occurred at SFN concentrations well below those required to inhibit polymerization of the microtubules (i.e. below those required to reduce the polymer mass). Specifically, concentrations of SFN greater than ~70 μM were required to appreciably reduce polymerization of the purified microtubules (supplementary Figure 1 is available at *Carcinogenesis* Online). In contrast, much lower concentrations of SFN suppressed the growing and shortening dynamics of the microtubules. The most potent effects of SFN on the dynamics of purified microtubules, as in cells (discussed below), were the suppression of the rate and extent of growth and shortening, which caused the microtubules to remain in a non-dynamic state the majority of the time (Table I). For example, 15 μM SFN, which did not reduce the microtubule polymer mass, reduced the rate and extent of growth and shortening of individual microtubules by 30 to ~57%. Microtubule dynamic instability is also characterized by the switching between growth and shortening at

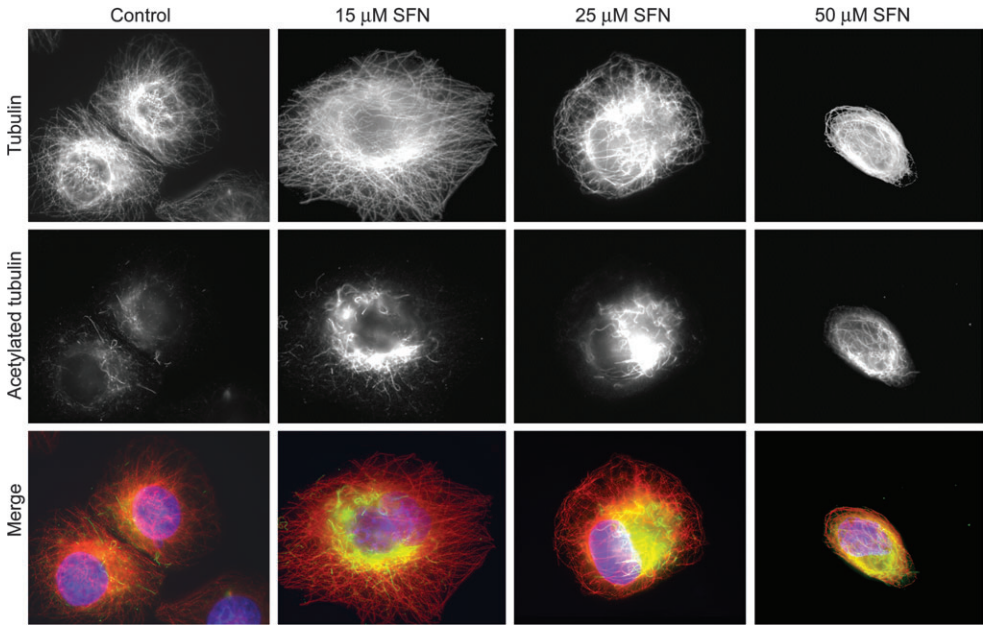

Fig. 5. SFN promotes acetylation of microtubules in MCF7-GFP-α-tubulin cells in a concentration-dependent manner. The panel of images designated 'Tubulin' are cytoplasmic microtubules in interphase control cells and cells treated with 15, 25 and 50 μM SFN for 24 h. The panel designated 'Acetylated tubulin' represents microtubules that have been extensively acetylated upon treatment with SFN compared with untreated controls. Tubulin is in red, acetylated tubulin is in green and nuclei (4′,6-diamidino-2-phenylindole) are in blue in the merged images.

microtubule ends, and SFN had little or no effect on the switching frequencies (catastrophe and rescue) between growth and shortening either in living cells or with purified microtubules (Table I), suggesting that it does not act on the mechanisms at the microtubule tips responsible for switching.

SFN inhibited cell proliferation and mitosis in MCF7-GFP-α-tubulin cells with half-maximal inhibition occurring at 26 and 13 μM, respectively. Inhibition occurred at prometaphase/metaphase and was accompanied by significant distortion of the mitotic spindles. However, no significant microtubule depolymerization was observed either by immunofluorescence microscopy of fixed cells at the IC_{50} for mitotic arrest or during imaging of microtubules in live cells (data not shown). Persistent mitotic arrest by SFN led to a time- and concentration-dependent induction of apoptosis (Figure 1D). While 15 μM SFN did not appreciably inhibit polymerization of purified microtubules or the organization, quantity or structure of microtubules in interphase or mitotic MCF7-GFP-α-tubulin cells, this concentration strongly suppressed the growth and shortening dynamics of the microtubules. Similar to the effects of SFN on purified microtubules, its principle effects on microtubules in living cells were the suppression of the length and rate of growth and shortening actions that greatly increased the fraction of time the microtubules remained in an attenuated or paused state (Table I). The microtubules were clearly stabilized by SFN as determined independently by staining with an antibody to acetylated α-tubulin (Figure 5). Thus, the effects of SFN on microtubule dynamic instability and turnover in cells are similar to its effects on steady-state microtubules composed solely of purified tubulin. Overall, the results indicate that the effects of SFN on microtubule dynamics in cells are a result of its direct action on the microtubules and are not due to modification of the soluble tubulin levels or to an action on any microtubule regulatory proteins.

How might SFN inhibit proliferation at mitosis?

Importantly, the ability of SFN to inhibit proliferation, arrest mitosis and induce apoptosis in MCF7-GFP-α-tubulin cells is similar to the way many of the more powerful microtubule-targeted anticancer drugs act [e.g. vinca alkaloids and taxanes (45–47)], by effective suppression of microtubule dynamics and stabilization of microtubules. The dynamics and turnover of microtubules increase many fold when cells enter mitosis. The rapid dynamics are critically important to construct the spindle and for the precise and time-sensitive segregation of the duplicated chromosomes into the daughter cells (35). Suppression of the dynamics and the resulting induction of mitotic arrest by microtubule-targeted antimitotic drugs lead to death of sensitive tumor cells by apoptosis (34,48). It is noteworthy that SFN's relatively strong ability to suppress dynamic instability and relatively weak ability to modulate the mass of assembled microtubule polymers are very similar to the actions of the vinca alkaloids and taxanes. Suppression of the growth and rapid shortening of spindle microtubules by these drugs results in an incomplete attachment of microtubules to chromosomes at their kinetochores, incomplete formation of metaphase spindles and a reduction in spindle tension, all of which are required for progression into anaphase and satisfaction of the metaphase checkpoint (49,50).

SFN, while less potent than the microtubule-targeted anticancer drugs, appears to act in a similar fashion. At the IC_{50} for inhibition of mitosis in MCF7-GFP-α-tubulin cells, SFN clearly prevented mitotic spindle progression from metaphase to anaphase since the anaphase/telophase to prometaphase/metaphase ratio was reduced by 85%. At the lowest effective concentrations, arrested spindles had a normal quantity of microtubules, but only ∼13% of the spindles in arrested mitotic cells were bipolar and contained uncongressed chromosomes (Figure 2C, arrowheads). Interestingly, most spindles were monopolar and a significant number of the chromosomes were not visibly attached to microtubules, unlike monopolar spindles induced by taxanes and vinca alkaloids (48). The unusual predominance of SFN-induced monopolar spindles (Figure 2E) suggests that SFN might also affect the function of a mitotic kinesin required for the development of bipolar spindles.

How might SFN modulate microtubule dynamics?

Most microtubule-targeted anticancer drugs have been shown to modulate microtubule dynamics by binding to specific sites in tubulin along microtubule surfaces or by end-poisoning mechanisms (29). Recent evidence has indicated that SFN may bind covalently to cysteine residues of proteins (51) and that it appears to bind covalently and with some selectively to tubulin in extracts of A549 tumor cells in parallel with its ability to inhibit cell proliferation (26). Here, we demonstrate that SFN affects the dynamic instability of microtubules

at steady state, conditions in which the free tubulin concentration is unchanging. Thus, its effects on dynamics are not brought about by SFN changing the availability of the assembly competent tubulin pool. More probably, its effects on dynamics are due to an action of SFN itself or SFN–tubulin complexes directly on tubulin in the microtubules. The binding of SFN to tubulin has been shown to alter tubulin's secondary and tertiary structures (26). Thus, one possibility is that SFN–tubulin complexes can incorporate at microtubule ends in a manner somewhat similar to colchicine–tubulin complexes, which dissociate very slowly once formed and stabilize the ends once they are incorporated (52). An alternative possibility is that SFN binds directly to exposed cysteine residues in tubulin along the microtubule surface or at its ends. These possibilities remain to be evaluated.

SFN as a possible anticancer agent

The chemopreventive and anticancer effects of SFN occur at concentrations that appear to be achievable in the diet (e.g. 0.5–25 μM for *in vitro* modulation of Phase I and Phase II enzymes, 0.1–300 μM for the cell cycle arrest and induction of apoptosis and 0.1–50 μM for inhibition of angiogenesis, reviewed in refs 12,13,53). Suppression of microtubule dynamics and inhibition of cell proliferation and mitosis in MCF7-GFP-α-tubulin cells also occur at concentrations that are achievable in the diet. Thus, the microtubule-targeted effects of SFN may play a role in its chemopreventive and anticancer ability. One possibility is that the consumption of cruciferous vegetables may selectively prevent and/or retard proliferation of precancerous, neoplastic and/or malignant cells during early stages of carcinogenesis because such cells may divide more rapidly than their normal counterparts and, therefore, be vulnerable to mitotic arrest (26,35).

Because the actions of SFN on microtubule dynamics resemble those of microtubule-targeted anticancer drugs, it is important to determine whether SFN might facilitate or interfere with conventional chemotherapy. If it does not interfere, an attractive possibility is that SFN may not only be useful for prevention of cancer but also for the treatment of cancer along with the commonly used conventional drugs. The use of agents, including those with low potency such as SFN, in combination with drugs that act by similar or different mechanisms, might provide increased efficacy while minimizing toxicity.

Supplementary material

Supplementary Figure 1 can be found at http://carcin.oxfordjournals.org/

Funding

California Breast Cancer Research Program dissertation award (12GB-0137 to O.A.); University of California Cancer Research Coordinating Committee (SB060145 to L.W.); National Institute of Health (NS13560, CA 57291).

Acknowledgements

We thank Mr Herbert Miller for the technical help.

Conflict of interest statement: None declared.

References

1. Zhang,Y.S. *et al*. (1992) A major inducer of anticarcinogenic protective enzymes from broccoli—isolation and elucidation of structure. *Proc. Natl Acad. Sci. USA*, **89**, 2399–2403.
2. Zhang,Y.S. *et al*. (2006) Vegetable-derived isothiocyanates: anti-proliferative activity and mechanism of action. *Proc. Nutr. Soc.*, **65**, 68–75.
3. Xu,C. *et al*. (2006) Inhibition of 7,12-dimethylbenz(a)anthracene-induced skin tumorigenesis in C57BL/6 mice by sulforaphane is mediated by nuclear factor E2-related factor 2. *Cancer Res.*, **66**, 8293–8296.
4. Singh,A.V. *et al*. (2004) Sulforaphane induces caspase-mediated apoptosis in cultured PC-3 human prostate cancer cells and retards growth of PC-3 xenografts *in vivo*. *Carcinogenesis*, **25**, 83–90.
5. Juge,N. *et al*. (2007) Molecular basis for chemoprevention by sulforaphane: a comprehensive review. *Cell. Mol. Life Sci.*, **64**, 1105–1127.
6. Ambrosone,C.B. *et al*. (2004) Breast cancer risk in premenopausal women is inversely associated with consumption of broccoli, a source of isothiocyanates, but is not modified by GST genotype. *J. Nutr.*, **134**, 1134–1138.
7. Verhoeven,D.T. *et al*. (1996) Epidemiological studies on brassica vegetables and cancer risk. *Cancer Epidemiol. Biomarkers Prev.*, **5**, 733–748.
8. Ye,L.X. *et al*. (2002) Quantitative determination of dithiocarbamates in human plasma, serum, erythrocytes and urine: pharmacokinetics of broccoli sprout isothiocyanates in humans. *Clin. Chim. Acta*, **316**, 43–53.
9. Hu,R. *et al*. (2004) *In vivo* pharmacokinetics and regulation of gene expression profiles by isothiocyanate sulforaphane in the rat. *J. Pharmacol. Exp. Ther.*, **310**, 263–271.
10. Hanlon,N. *et al*. (2008) Absolute bioavailability and dose-dependent pharmacokinetic behaviour of dietary doses of the chemopreventive isothiocyanate sulforaphane in rat. *Br. J. Nutr.*, **99**, 559–564.
11. Cornblatt,B.S. *et al*. (2007) Preclinical and clinical evaluation of sulforaphane for chemoprevention in the breast. *Carcinogenesis*, **28**, 1485–1490.
12. Conaway,C.C. *et al*. (2002) Isothiocyanates as cancer chemopreventive agents: their biological activities and metabolism in rodents and humans. *Curr. Drug Metab.*, **3**, 233–255.
13. Zhang,Y.S. (2004) Cancer-preventive isothiocyanates: measurement of human exposure and mechanism of action. *Mutat. Res.*, **555**, 173–190.
14. Dinkova-Kostova,A.T. *et al*. (2008) Direct and indirect antioxidant properties of inducers of cytoprotective proteins. *Mol. Nutr. Food Res.*, **52**, 1–11.
15. Jeffery,E.H. *et al*. (2008) Translating knowledge generated by epidemiological and *in vitro* studies into dietary cancer prevention. *Mol. Nutr. Food Res.*, **52**, 12–23.
16. Maheo,K. *et al*. (1997) Inhibition of cytochromes P-450 and induction of glutathione S-transferases by sulforaphane in primary human and rat hepatocytes. *Cancer Res.*, **57**, 3649–3652.
17. Brooks,J.D. *et al*. (2001) Potent induction of phase 2 enzymes in human prostate cells by sulforaphane. *Cancer Epidemiol. Biomarkers Prev.*, **10**, 949–954.
18. Munday,R. *et al*. (2004) Induction of phase II detoxification enzymes in rats by plant-derived isothiocyanates: comparison of allyl isothiocyanate with sulforaphane and related compounds. *J. Agric. Food Chem.*, **52**, 1867–1871.
19. Nestle,M. (1997) Broccoli sprouts as inducers of carcinogen-detoxifying enzyme systems: clinical, dietary, and policy implications. *Proc. Natl Acad. Sci. USA*, **94**, 11149–11151.
20. Jackson,S.J. *et al*. (2007) Sulforaphane suppresses angiogenesis and disrupts endothelial mitotic progression and microtubule polymerization. *Vascul. Pharmacol.*, **46**, 77–84.
21. Woo,K.J. *et al*. (2007) Sulforaphane suppresses lipopolysaccharide-induced cyclooxygenase-2 (COX-2) expression through the modulation of multiple targets in COX-2 gene promoter. *Int. Immunopharmacol.*, **7**, 1776–1783.
22. Myzak,M.C. *et al*. (2004) A novel mechanism of chemoprotection by sulforaphane: inhibition of histone deacetylase. *Cancer Res.*, **64**, 5767–5774.
23. Gamet-Payrastre,L. (2006) Signaling pathways and intracellular targets of sulforaphane mediating cell cycle arrest and apoptosis. *Curr. Cancer Drug Targets*, **6**, 135–145.
24. Jackson,S.J. *et al*. (2004) Sulforaphane inhibits human MCF-7 mammary cancer cell mitotic progression and tubulin polymerization. *J. Nutr.*, **134**, 2229–2236.
25. Jackson,S.J. *et al*. (2004) Sulforaphane: a naturally occurring mammary carcinoma mitotic inhibitor, which disrupts tubulin polymerization. *Carcinogenesis*, **25**, 219–227.
26. Mi,L. *et al*. (2008) Covalent binding to tubulin by isothiocyanates: a mechanism of cell growth arrest and apoptosis. *J. Biol. Chem.*, **283**, 22136–22146.
27. Desai,A. *et al*. (1997) Microtubule polymerization dynamics. *Annu. Rev. Cell Dev. Biol.*, **13**, 83–117.
28. Nogales,E. (2001) Structural insights into microtubule function. *Annu. Rev. Biophys. Biomol. Struct.*, **30**, 397–420.
29. Jordan,M.A. *et al*. (2008) Microtubule dynamics: mechanisms and regulation by microtubule-associated proteins and drugs *in vitro* and in cells. In Fojo,T. (ed.) *The Role of Microtubules in Cell Biology, Neurobiology, and Oncology.* Humana Press, Totowa, NJ, pp. 47–81.
30. Mitchison,T.J. *et al*. (1984) Dynamic instability of microtubule growth. *Nature*, **312**, 237–242.
31. Grishchuk,E.L. *et al*. (2005) Force production by disassembling microtubules. *Nature*, **438**, 384–388.
32. Rudner,A.D. *et al*. (1996) The spindle assembly checkpoint. *Curr. Biol.*, **8**, 773–780.
33. Kelling,J. *et al*. (2003) Suppression of centromere dynamics by Taxol in living osteosarcoma cells. *Cancer Res.*, **63**, 2794–2801.

34. Okouneva,T. *et al*. (2003) The effects of vinflunine, vinorelbine, and vinblastine on centromere dynamics. *Mol. Cancer Ther.*, **2**, 427–436.
35. Jordan,M.A. *et al*. (2004) Microtubules as a target for anticancer drugs. *Nat. Rev. Cancer*, **4**, 253–265.
36. Jordan,M.A. *et al*. (2007) How do microtubule-targeted drugs work? An overview. *Curr. Cancer Drug Targets*, **7**, 730–742.
37. Webster,D.R. *et al*. (1989) Microtubules are acetylated in domains that turn over slowly. *J. Cell Sci.*, **92**, 57–65.
38. Wilson,L. *et al*. (1985) Taxol stabilization of microtubules *in vitro*: dynamics of tubulin addition and loss at opposite microtubule ends. *Biochemistry*, **24**, 5254–5262.
39. Panda,D. *et al*. (1996) Differential effects of vinblastine on polymerization and dynamics at opposite microtubule ends. *J. Biol. Chem.*, **271**, 29807–29812.
40. Bunker,J.M. *et al*. (2004) Modulation of microtubule dynamics by tau in living cells: implications for development and neurodegeneration. *Mol. Biol. Cell*, **15**, 2720–2728.
41. Kamath,K. *et al*. (2003) Suppression of microtubule dynamics by epothilone B in living MCF7 cells. *Cancer Res.*, **63**, 6026–6031.
42. Panda,D. *et al*. (1995) Kinetic stabilization of microtubule dynamics at steady state by tau and microtubule-binding domains of tau. *Biochemistry*, **34**, 11117–11127.
43. Walker,R.A. *et al*. (1988) Dynamic instability of individual microtubules analyzed by video light microscopy: rate constants and transition frequencies. *J. Cell Biol.*, **107**, 1437–1448.
44. Jordan,M.A. *et al*. (1986) Identification of a distinct class of vinblastine binding sites on microtubules. *J. Mol. Biol.*, **187**, 61–73.
45. Wilson,L. *et al*. (1999) Modulation of microtubule dynamics by drugs: a paradigm for the actions of cellular regulators. *Cell Struct. Funct.*, **24**, 329–335.
46. Mollinedo,F. *et al*. (2003) Microtubules, microtubule-interfering agents and apoptosis. *Apoptosis*, **8**, 413–450.
47. Jordan,M.A. (2002) Mechanism of action of antitumor drugs that interact with microtubules and tubulin. *Curr. Med. Chem.*, **2**, 1–17.
48. Ngan,V. *et al*. (2001) Mechanism of mitotic block and inhibition of cell proliferation by the semisynthetic Vinca alkaloids vinorelbine and its newer derivative vinflunine. *Mol. Pharmacol.*, **60**, 225–232.
49. Li,X. *et al*. (1995) Mitotic forces control a cell-cycle checkpoint. *Nature*, **373**, 630–632.
50. Nicklas,R.B. *et al*. (1995) Kinetochore chemistry is sensitive to tension and may link mitotic forces to a cell cycle checkpoint. *J. Cell Biol.*, **130**, 929–939.
51. Mi,L. *et al*. (2007) The role of protein binding in induction of apoptosis by phenethyl isothiocyanate and sulforaphane in human non-small lung cancer cells. *Cancer Res.*, **67**, 6409–6416.
52. Skoufias,D. *et al*. (1992) Mechanism of inhibition of microtubule polymerization by colchicine: inhibitory potencies of unliganded colchicine and tubulin-colchicine complexes. *Biochemistry*, **31**, 738–746.
53. Fimognari,C. *et al*. (2007) Sulforaphane as a promising molecule for fighting cancer. *Mutat. Res.*, **635**, 90–104.

Received August 31, 2008; revised October 10, 2008;
accepted October 10, 2008